Evaluating Protection System Performance for a Real-World Weak Grid Area With High Inverter-Based Resources

Abu Shouaib Hasan,[1] Yaswanth Velaga,[1] Jing Wang,[1] Lang Chen,[2] Joseph Dubeau,[2] Andrew Arana[2]
[1]National Laboratory of the Rockies, Colorado 80401, USA
[2]Florida Power and Light, Florida 33155, USA
{AbuShouaib.Hasan, YaswanthNag.Velaga, jing.wang}@nrel.gov, {lang.chen, Joseph.Dubeau, andrew.arana}@fpl.com

***Abstract*—This paper evaluates an existing protection scheme implemented in a real-world weak grid area with a high penetration of inverter-based resources (IBRs). The study aims to assess the reliability and adequacy of protection schemes originally designed for traditional synchronous machine systems and determine whether they can continue to operate reliably in systems with high levels of IBRs. Hardware relays are tested using a controller-hardware-in-the-loop setup. PSCAD electromagnetic transient simulation with an IBR original equipment manufacturer black-box model is used to perform fault studies and generate COMTRADE data, which are replayed by a real-time digital simulator (RTDS) to feed input to the hardware relays. Three scenarios are analyzed: normal operation, an N-1 contingency, and an IBR-only scenario. The evaluation results reveal the following: 1) the protection scheme remains reliable under normal conditions and N-1 contingencies and 2) in IBR-only scenarios, differential protection (87L) continues to operate reliably, whereas local protection elements, such as distance and directional elements, fail because of the lack of regulated negative sequence current contributed by IBRs. These findings provide utilities with valuable insights for improving their protection systems in high-IBRs.**

I. Introduction

The recent North American Electric Reliability Corporation Relay Misoperation report indicates incorrect setting/logic/design errors are still the main causes of relay misoperation, and among all the events, 5% are caused by inverter-based-resources (IBRs) [1]. As of today, relay misoperation caused solely by IBRs are still rare because in most situations the traditional synchronous machines still contribute fault current together with the IBRs. However, with the rapid displacement of synchronous machines by IBRs, the relay misoperations caused by IBRs will become more frequent. Therefore, much research effort has been devoted to understand the fault characteristics of IBRs and especially how they will impact the protection system/schemes that are originally designed for systems with synchronous machines.

Studies in [2], [3], [4], [5] investigate how various IBR modeling and control aspects affect transmission line protection elements, such as distance elements, directional elements, and fault identification logic (FID). Because those elements rely on regulated negative sequence current injection, references [6], [7] study the benefits of including negative sequence current control in IBRs to produce consistent fault current that is IEEE 2800-2022 compliant so the transmission line protection elements can operate reliably. Because momentary cessation may cause IBRs to stop injecting fault current, a study was performed to determine the minimal time at which IBRs should inject fault current so the protection relay can see enough current and pick up [8]. A recent report from a utility industry summarizes the key challenges of protection systems with IBRs because of the nontraditional fault current with multiple real-world relay misoperation examples [9]. A separate report conducted a gap analysis based on a comprehensive literature review and expert interviews, concentrating on the effects of grid-forming (GFM) IBRs on protection systems [10]. Furthermore, SEL outlined a set of solutions that is applied in systems with IBRs using the series of SEL protection relays [11], and IEEE Power System Relaying and Control Committee working group C32 has a white paper describing protection challenges and practices for transmission systems with high IBRs [12]. The impacts of various wind turbine generators on negative sequence quantities-based protection elements ($50Q$, $51Q$, and $67Q$) are studied in [13] to understand the potential protection misoperation issues, identify the causes, and propose potential solutions. Similarly, the impact of IBRs on protective relay elements, such as distance and direction elements, is studied to further understand how IBRs negatively impact the performance of traditional protection schemes [14].

However, there are a limited number of works that properly evaluate the real-world protection system challenges with high IBRs and highlight exact issues to be resolved. In particular, the methodology to perform those evaluation studies is not yet studied or well understood. Therefore, this paper addresses the research gap and the main contributions of this paper can be summarized as follows: i) it develops a generic framework to perform protection study evaluation using a real-world system, addressing the gap of lack of an available power system model with accurate IBR representation and systematic evaluation approach; ii) it highlights the exact issues of lack of negative sequence on protection elements; and iii) it validates the impacts using a real-world network and provides trustworthy analysis and recommendations for protection engineers to understand the potential misoperation, identify the root cause,

This work was authored by the National Laboratory of the Rockies for the U.S. Department of Energy (DOE), operated under Contract No. DE-AC36-08GO28308. Support for the work was also provided by Florida Power and Light under Agreement Number CRD-23-24406-0. The views expressed in the article do not necessarily represent the views of the DOE or the U.S. Government.

979-8-3315-8138-1

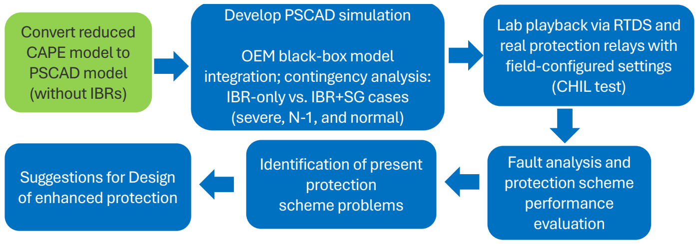

Fig. 1: Framework of the proposed protection system study and suggest enhanced protection strategies.

II. Overview of the Protection System Under Study

A. Protection Study Methodology

Fig. 1 shows the framework of the proposed protection system study. The full CAPE model is reduced to include only the weak grid area of interest; the reduced CAPE model is then manually developed in a PSCAD electromagnetic transient simulation tool. Comprehensive modeling validation is performed for each modeling step, including comparing the fault current levels with LG, LL and LLG faults and validating the relay responses with those faults. Once the PSCAD model is validated, the IBR black-box model provided by the original equipment manufacturer (OEM) is integrated. Three scenarios are considered: the normal condition, the N-1 contingency, and the IBR-only scenarios. The PSCAD model is used to run the fault studies with all the considered scenarios; the COMTRADE data from the PSCAD simulation are saved and replayed in a real-time digital simulator (RTDS). The hardware relays are connected to the RTDS and an automatic Python script is developed to run all the fault scenarios and evaluate the relay responses. Then, we identify the protection issues and make suggestions for enhanced protection to improve the protection system reliability and security.

B. Power System Model for Fault Study

The full CAPE model was received from the utility partner but was too large to perform the fault study for the weak grid area of interest. Therefore, the full CAPE model was reduced to a smaller system that contains the weak grid area with high IBRs. The main challenges faced during this model reduction are as follows: 1) there is no good practice to equivalent the area with IBRs; 2) there are floating transformer neutral issues; and 3) the current of non-faulted phase is not the same between the full and reduced model for unbalanced faults because of the presence of IBRs in the reduced network. Extensive troubleshooting was performed to resolve those challenges with assistance from the CAPE technical support team. Finally, the fault current comparison and COMTRADE data replay in RTDS and hardware relay shows good agreement between the reduced and full CAPE model. The next step is to manually build the reduced CAPE model in PSCAD; the main challenge is to calculate the zero-sequence impedance for all the components, including voltage source, lines, and transformers. Legacy two- and three-winding transformer models zero sequence in PSCAD can't be modified through parameters. Therefore, a custom transformer model from the PSCAD library is used to represent two-winding and three-winding transformers. Zero-sequence parameters are derived from the

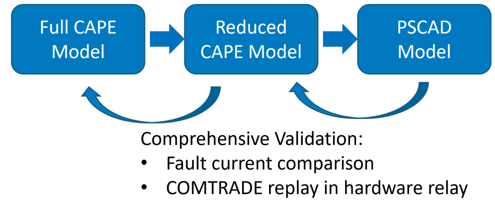

Fig. 2: Process of developing the PSCAD model

reduced CAPE model for the PSCAD model.

Because of the limited space of this paper, the validation results are not included. Fig. 2 shows the process of developing the PSCAD model, and Fig. 3 shows the single-line diagram of the system under study. Note the IBR plant with a 75-megawatt (MW) solar and 75-MW battery energy storage system is connected at Bus 11, and the transmission lines under fault study and protection scheme evaluation are between Bus 10 and Bus 11 ($L1$) and between Bus 11 and Bus 12 ($L2$). Lines $L1$ and $L2$ are 113 miles and 60 miles long, respectively.

C. Black-Box Grid-Following Inverter Model

The black-box model provided by the inverter vendor are then integrated into the PSCAD power system model. A BC unbalanced fault is applied to understand the fault characteristics of the grid-following (GFL) inverter. The fault responses are indicated in Fig. 4, which shows the active component of positive sequence current, $I_{1\mathrm{A}} := |I_1|\cos(\angle V_1 - \angle I_1)$; the reactive component of the positive sequence current, $I_{1\mathrm{R}} := |I_1|\sin(\angle V_1 - \angle I_1)$; the active component of the negative sequence current, $I_{2\mathrm{A}} := |I_2|\cos(\angle V_2 - \angle I_2)$; and the reactive component of the negative sequence current, $I_{2\mathrm{R}} := |I_2|\sin(\angle V_2 - \angle I_2)$. According to IEEE 2800-2022, if the IBR injects by default q-priority current and negative sequence current lead negative sequence voltage 90 degrees, we have $I_{2\mathrm{A}} := 0$ and $I_{2\mathrm{R}} := -|I_2|$. If the fault is severe, then $I_{1\mathrm{A}} := 0$ and $I_{1\mathrm{R}} := |I_1|$. The GFL inverter fault responses indicate the IBRs are not IEEE 2800-2022 negative sequence current compliant. In addition, the IBR fault currents are oscillatory and low. Those fault characteristics will pose challenges to protection relays under IBR-only scenarios.

III. Fault Study and Protection Scheme Evaluation

A. Use Case Study

Based on the discussion with our utility partner, several contingencies are identified for Lines $L1$ and $L2$. Table I summarizes the $L1$ protection study scenarios and simulated fault types. All the contingency scenarios are grouped under three subcategories: normal (gray), N-1 contingency (blue), and IBR-only source (red). When Line $L2$ is out of service, it creates a condition in which IBR is the only source and therefore classified as IBR to differentiate from other N-1 contingencies. Protection studies are primarily focused on three faults: single-line-to-ground fault, phase-to-phase fault, and double-line-to-ground fault. Three fault locations are considered: close-in from $L1$ (5%), end of Zone 1 from $L1$ (80%), and remote close-in from $L1$ (95%). For $L2$, the contingency scenarios are the same except that the IBR case, Line $L1$ is out of service. Bolted fault is applied for all the scenarios.

979-8-3315-8138-1

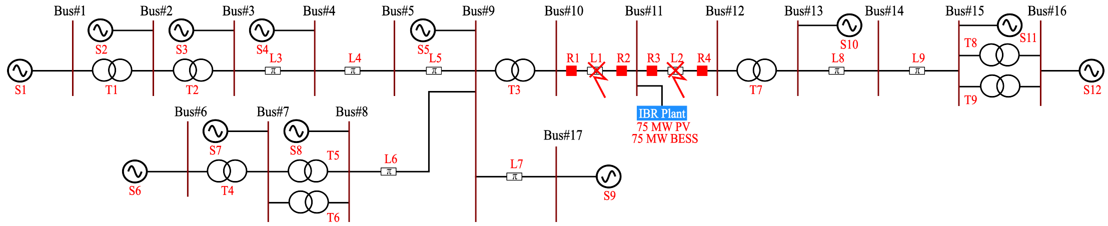

Fig. 3: Single-line diagram of the power system under study

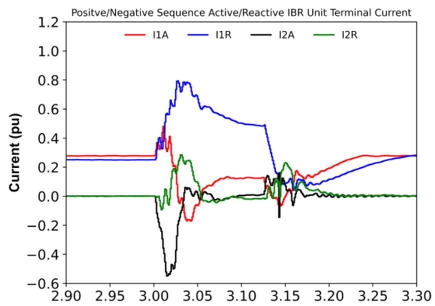

Fig. 4: GFL inverter fault current response under BC fault.

TABLE I: List of All the Tested Scenarios for $L1$

Contingency	5% of the $L1$			80% of the $L1$			95% of the $L1$		
	AG	BC	BCG	AG	BC	BCG	AG	BC	BCG
All in Service	✓	✓	✓	✓	✓	✓	✓	✓	✓
S5	✓	✓	✓	✓	✓	✓	✓	✓	✓
S10	✓	✓	✓	✓	✓	✓	✓	✓	✓
L5	✓	✓	✓	✓	✓	✓	✓	✓	✓
L6	✓	✓	✓	✓	✓	✓	✓	✓	✓
L8	✓	✓	✓	✓	✓	✓	✓	✓	✓
L2	✓	✓	✓	✓	✓	✓	✓	✓	✓

B. Laboratory Controller Hardware-in-the-Loop Setup

Fig. 5 shows the laboratory controller hardware-in-the-loop (CHIL) setup for the hardware relay testing. The two relays on the left are used for the Line $L1$ protection, and the two on the right are for the $L2$ protection. The relay .rdb setting files are provided by the utility partner and three field event data are used to validate the relay settings, CT and PT ratios, to replicate the field setup for the relays. Instantaneous voltage and current waveforms were recorded from the CTs and PTs within the PSCAD model and stored in COMTRADE format for each relay. These COMTRADE files were used as input signals to the relays through the RTDS platform. The RTDS was interfaced with the relays via GTAO cards, enabling real-time playback of the simulated signals. Line protection relays are connected through fiber-optic cable for differential protection to emulate field deployment. This ensured the laboratory CHIL environment mirrored the actual field implementation, providing a robust platform for validating relay performance under realistic operating conditions.

IV. Evaluation of Protection System Performance

A. Evaluation Results of Transmission Line $L1$ with GFL IBR

All the scenarios defined in Table I are evaluated. The important protection relay elements in the four relays are line differential element $87L$, Mho phase and ground distance elements $21MP$ and $21MG$, directional element $32Q/32V$, and differential-based FID. Both relays (R_1 and R_2) operate

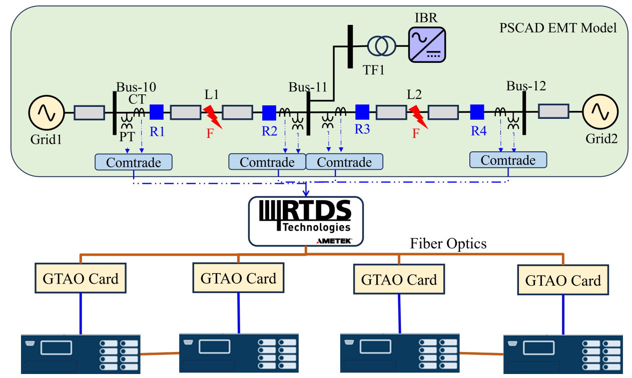

Fig. 5: Diagram of the laboratory relay CHIL testing setup.

reliably under normal conditions and N-1 contingencies because there is still a significant amount of negative sequence current contributed by the traditional synchronous machines. For the GFL IBR-only scenario, Relay R_1 operates reliably; for Relay R_2, the differential elements operate reliably and respond within 2 cycles, and the $87FID$ also operates reliably. Example results for normal operation, N-1 contingency, and IBR only scenario under AG and BC faults are presented in Fig. 7. The start of each bar indicates when the digital element is activated. However, the directional elements (e.g., $32Q$) and distance element that rely on the regulated negative sequence current (magnitude and $\angle I_2$ leads $\angle V_2$ by $90°$) can't assert. More analysis is given below.

As discussed in Section II-C, GFL IBRs do not provide regulated negative sequence current for unbalanced faults. It is important to understand specific negative sequence elements that are affected by unregulated negative sequence current from GFL IBRs. The $32Q$-based directional logic requires Z_2 to be below its threshold Z_{2FTH} to indicate a forward fault; however, Z_2 is above this threshold during the IBR-only scenario. Fig. 6 shows the Z_2 with forward and reverse thresholds. At the onset of fault, Z_2 is oscillatory, which is caused by the non-steady phase angle between I_2 and V_2 (a behavior is shown in Table II). Because of the oscillation and I_2 not leading V_2 by $90°$, Z_2 has a very oscillatory response and cannot indicate the correct fault direction. Note the $32Q$ element did not assert in all the tested IBR-only cases.

TABLE II: The Phase Angle of $\angle I_2$ - $\angle V_2$ Under a BC Fault

	1^{st} cycle	2^{nd} cycle	3^{rd} cycle
Normal	98.81°	98.81°	98.81°
N-1	91.9°	98.91°	91.9°
GFL IBR only	171.11°	−137.51°	−66.5°

For the line-to-ground (e.g., AG) fault, the utility partner uses both negative-sequence– and zero-sequence-based voltage polarized directional elements, denoted as $32Q$ and $32V$,

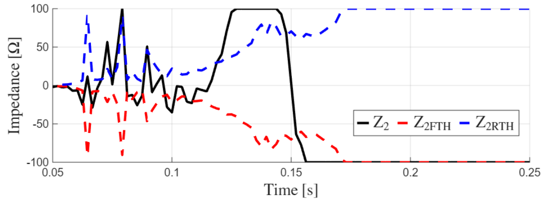

Fig. 6: Negative sequence directional element impedance vs. forward/reverse threshold (IBR-only).

respectively. The preferred directional decision logic follows the QV order, prioritizing $32Q$ when negative sequence current is present and above its threshold; in this case, $32V$ is inhibited from asserting $32G$ until relay internal logic determines negative sequence quantities are not available and switches to the zero-sequence voltage polarized element. In addition, the $Z1G/Z2G$ element could not assert initially because it was supervised by the $32Q$ element. After about 3 cycles, the I_2 current dropped below its threshold, allowing the $Z1G/Z2G$ element to assert based on the $32V$ element as shown in Fig. 7a.

For the line-to-line (e.g., BC) fault, initially I_2 activated $32QE$; however, $F32Q$ could not assert because I_2 doesn't lead V_2 by 90°. In line-to-line faults, the $32P$ element serves as the directional decision element and is typically coordinated with $32Q$. To enable $Z1P/Z2P$, $32P$ provides directionality, but tripping decisions are ultimately governed by threshold-hold comparators (e.g., Mho characteristic comparator and line-to-line current comparator) associated with the selected distance characteristic. In these tests, $Z1P/Z2P$ did not assert because of the absence of a regulated I_2 contribution and low fault current magnitudes as shown in Fig. 7b. In addition, the expected negative sequence phasor relationship, $\angle I_2$ leading $\angle V_2$ by approximately 90° under normal and $N-1$ contingency conditions, did not hold in the IBR-only scenario because I_2 was not regulated as shown in Table II. The $Z1P/Z2P$ elements also did not assert during BCG faults because of the same underlying limitations: the absence of a regulated I_2 contribution from the IBR and insufficient fault current.

The performance of Relay R_2 under various fault scenarios in a GFL IBR-only scenario is summarized in Table III. Table IV provides the brief description of protection elements mentioned in Table III. For ground faults, three fault locations are considered and, for each fault location, two IBR power references (0.1 p.u. and 0.9 p.u.) are simulated. As discussed in Section IV-A, the preferred ground directional logic is set to order QV. When the relay internal logic determines negative sequence quantities are not available, it switches to the zero-sequence voltage polarized element. From Table III, negative sequence elements are enabled ($32QE$) momentarily for about half a cycle. Eventually, ground fault is detected by distance elements after 4.875 cycles and 3.375 cycles for 5% fault location with 0.1 p.u. and 0.9 p.u. P_{ref}, respectively. Fault detection is delayed because the relay checks for negative sequence quantities and then takes approximately 1-2 cycles to switch from negative sequence to zero sequence. At higher power level (0.9 p.u.), fault detection delay is shorter because fault current magnitude is higher and faster to go beyond magnitude threshold comparators. As the fault gets farther from the remote end (95% fault location) to close in (5%),

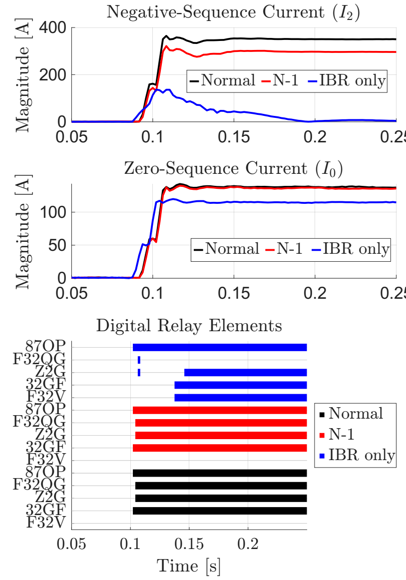

(a) AG Fault

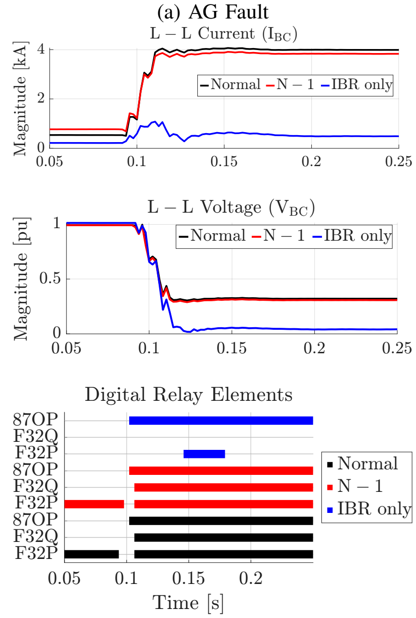

(b) BC fault

Fig. 7: Negative sequence current, zero-sequence current, and relay element binary outputs.

fault detection time decreases because fault current magnitude is higher as the fault gets close and relay makes its decision faster. It is important to remember there are no additional delays set for distance elements. For line-to-line faults, relay depends primarily on negative sequence quantities. Table III shows $32QE$ asserts momentarily for about half a cycle and de-asserts later. Phase ($32P$) and negative sequence current polarized ($32Q$) directional elements supervise the phase distance elements. When $Zload$ is enabled, the relay disables the $32P$ element from operating [15]. The main reason relay failed to detect a fault is because Z_2 to be above its threshold Z_{2FTH}, which caused $32QF$ (negative sequence forward directional element) to not assert, blocking the distance elements from asserting. From Table III, the relay failed to detect line-to-line and line-to-line-to-ground faults at three fault locations

TABLE III: Summary of Relay R_2's Performance Under GFL IBR-Only Scenarios

Element	**AG – fault** 5% - 0.1 p.u.	**AG – fault** 5% - 0.9 p.u.	**AG – fault** 80% - 0.1 p.u.	**AG – fault** 80% - 0.9 p.u.	**AG – fault** 95% - 0.1 p.u.	**AG – fault** 95% - 0.9 p.u.
Z1G/Z2G/F32Q/ F32GF assertion time (cycle)	4.875 (Based on $F32V$)	3.375 (Based on $F32V$)	3.0 (Based on $F32V$)	2.375 (Based on $F32V$)	3.0 (Based on $F32V$)	1.5 (Based on $F32V$)
32QE assertion time (cycle)	0.375 (De-asserted after 0.05 sec.)	0.625 (De-asserted after 0.023 sec.)	0.625 (De-asserted after 0.05 sec.)	0.875 (De-asserted after 0.025 cycle)	0.375 (De-asserted after 0.07 sec.)	0.75 (De-asserted after 0.023 sec.)
32VE assertion time (cycle)	0.25	0.375	0.25	0.5	0.25	0.375
Element	**BC – fault** 5% - 0.1 p.u.	**BC – fault** 80% - 0.1 p.u.	**BC – fault** 95% - 0.1 p.u.	**BCG – fault** 5% - 0.1 p.u.	**BCG – fault** 80% - 0.1 p.u.	**BCG – fault** 95% - 0.1 p.u.
Z1P/Z2P/F32Q assertion time (cycle)	Failed Z_2 above Z_{2FTH}	Failed Z_2 above Z_{2FTH}	Failed Z_2 above Z_{2FTH}	Failed Z_2 above Z_{2FTH}	Failed Z_2 above Z_{2FTH}	Failed Z_2 above Z_{2FTH}
32QE assertion time (cycle)	0.5 (De-asserted after 0.08 sec.)	0.5 (De-asserted after 0.07 sec.)	0.5 (De-asserted after 0.07 sec.)	0.5 (De-asserted after 0.08 sec.)	0.5 (De-asserted after 0.06 sec.)	0.5 (De-asserted after 0.06 sec.)

TABLE IV: Explanation of Relay Elements

Variable	Description
Z1P/Z1G	Zone-1 pickup using either the Mho or quad phase/ground elements
Z2P/Z2G	Zone-2 pickup using either the Mho or quad phase/ground elements
F32Q/GF/QE/VE	Forward direction declaration of the 32QG/32GF /32QE/32VF element

because of the negative sequence current issue.

B. Evaluation Results of Transmission Line L2

Transmission Line $L2$ is significantly shorter, approximately half the length of Transmission Line $L1$. Consequently, $L2$ exhibits lower positive and zero-sequence impedance magnitudes, whereas the corresponding sequence impedance angles remain nearly identical to those of $L1$. Because the negative sequence directional element impedance depends on the I_2–V_2 phasor relationship—and given that the IBR does not provide a regulated I_2—the directional element behavior for $L2$ mirrors that of $L1$. For line-to-ground faults under IBR-only scenarios, Relay R_3 demonstrated the same response as Relay R_2 because both rely on identical directional elements. In the case of line-to-line and line-to-line-to-ground faults, although $L2$ has a lower impedance, the IBR current output is constrained by its internal controller. As a result, the fault current magnitude for $L2$ remained below the pickup threshold, preventing reliable operation of the phase distance elements. Similar to the observations on $L1$, the $Z1P/Z2P$ elements did not assert during $L2$ fault tests because of the absence of a regulated negative sequence current contribution and the overall low fault current magnitudes.

V. Conclusion

This paper evaluates the protection system performance of a real-world weak grid area with GFL IBRs. For normal and N-1 contingency scenarios, the existing protection schemes operate effectively and reliably because a good amount of fault current is contributed by traditional synchronous machines. However, when IBR is the only source contributing fault current, the differential element still operates reliably, but the distance and directional elements that rely on the regulated negative sequence current and/or overcurrent misoperate. The affected protection relay elements are i) $32Q$ and ii) $Z1P/Z2P/Z1G/Z2G$. The inability of these elements to assert correctly stems from the lack of consistent I_2–V_2 phasor relationships and insufficient negative sequence current and fault current. These results underscore the need for enhanced directional algorithms, inverter-aware fault detection schemes, and enhanced supervision elements/logic that accounts for the dynamic behavior of GFL IBRs. Future work will include GFM IBRs for the study and design of enhanced protection schemes.

Acknowledgment

We would like to thank Siddharth Pant and Pooja Gupta from GE Vernova as well as the Siemens CAPE Technical Support Team for their valuable support to this work.

References

[1] "Protection system misoperations," in *2025 NERC Relay Misoperation Report*. NERC report, 2025.
[2] S. Chakraborty *et al.*, "Studying the impact of ibr modeling on the commonly applied transmission line protective elements," in *2024 IEEE Energy Conversion Conference and Expo (ECCE)*. IEEE, 2024.
[3] H. P. Pinheiro *et al.*, "Analysis of line distance elements for various ibr controllers and system conditions," *Electric Power System Research*, vol. 252, pp. 1–7, 2026.
[4] J. Wang *et al.*, "A comprehensive study of the impact of inverter-based resource (ibr) modeling and control on protection relay elements," in *PROTECT-IT Report*. NREL Technical report, 2025.
[5] A. S. Hasan and R. Fan, "Protecting inverter-based resources: Transformer configuration impacts and incremental focused directional protection enhancements," in *2025 IEEE Green Technologies Conference (GreenTech)*. IEEE, 2025.
[6] P. Pinheiro, S. Chakraborty, R. Bainy, H. Lei, B. K. Johnson, A. Alomari, S. Manson, J. Wang, R. Mahmud, A. Hoke, and C. J. Cruse, "Benefits and Recommendations for Using Classic Protection Functions in Transmission Lines Interfacing IBRs Compliant to IEEE 2800," in *2024 Grid of the Future Symposium*. Raleigh: CIGRE, 2024.
[7] J. B. B. M. Davi, M. Oleskovicz, and V. F. Lopes, "Study on ieee 2800-2022 standard benefits for transmission line protection in the presence of inverter-based resources," *Electric Power System Research*, vol. 220, pp. 1–9, 2023.
[8] S. Chakraborty *et al.*, "Studying the impact of momentary cessation of ibrs compliant with ieee std. 2800-2022 on transmission line protection elements," in *2025 IEEE PESGM*. IEEE, 2025.
[9] A. Saeed, M. Jensen, M. A. Zamani, and T. Raffield, "Utilities perspective on protection challenges with high ibr penetration," in *2019 IEEE 46th Photovoltaic Specialists Conference (PVSC)*. Sandia National Laboratory Report, 2025, pp. 1–41.
[10] U. Muenz *et al.*, "Protection of 100% inverter-dominated power systems with grid-forming inverters and protection relays – gap analysis and expert interviews," in *Sandia National Laboratory Report*, 2024.
[11] R. McDaniel, R. Chowdhury, K. Zimmerman, and B. Cockerham, "Applying sel relays in systems with inverter-based resources," in *SEL Application Guide*, vol. 1, no. AG2021-37. SEL Report, 2021.
[12] M. Nagpal *et al.*, "Protection challenges and practices for interconnecting inverter based resources to utility transmission systems," in *Power System Relaying and Control Committee Report of Working Group C32*. IEEE, pp. 1–70.
[13] A. Haddadi *et al.*, "Impact of inverter-based resources on negative sequence quantities-based protection elements," *IEEE Tran. Power Delivery*, vol. 36, no. 1, pp. 289–298, 2021.
[14] A. Haddadi, E. Farantatos, I. Kocar, and U. Karaagac, "Impact of inverter based resources on system protection," *Energise*, vol. 14, no. 1050, pp. 1–21, 2021.
[15] R. Chowdhury and N. Fischer, "Transmission Line Protection for Systems With Inverter-Based Resources."